

Simplicial models of social contagion

Iacopo Iacopini,^{1,*} Giovanni Petri,^{2,3} Alain Barrat,^{4,2} and Vito Latora^{1,5,6,7}

¹*School of Mathematical Sciences, Queen Mary University of London, London E1 4NS, United Kingdom*

²*ISI Foundation, Via Chisola 5, 10126 Turin, Italy*

³*ISI Global Science Foundation, 33 W 42nd St 10036 New York NY, United States*

⁴*Aix Marseille Univ, Université de Toulon, CNRS, CPT, Marseille, France*

⁵*The Alan Turing Institute, The British Library, London NW1 2DB, UK*

⁶*Dipartimento di Fisica ed Astronomia, Università di Catania and INFN, I-95123 Catania, Italy*

⁷*Complexity Science Hub Vienna (CSHV), Vienna, Austria*

(Dated: April 4, 2022)

Complex networks have been successfully used to describe the spreading of a disease between the individuals of a population. Conversely, pairwise interactions are often not enough to characterize processes of social contagion, such as opinion formation or the adoption of novelties, where a more complex dynamics of peer influence and reinforcement mechanisms is at work. We introduce here a high-order model of social contagion in which a social system is represented by a simplicial complex and the contagion can occur, with different transmission rates, over the links or through interactions in groups of different sizes. Numerical simulations of the model on synthetic simplicial complexes and analytical results highlight the emergence of novel phenomena, such as the appearance of an explosive transition induced by the high-order interactions.

Complex networks describe well the connectivity of systems of various nature [1, 2] and are widely used as the underlying social structure on which dynamical processes occur [3, 4], such as disease spreading [5], diffusion and adoption of innovation [6–8] and opinion formation [9]. In particular, when modeling epidemic spreading in a population [5], the transmission between infectious and healthy individuals are typically assumed: (i) to occur in a pairwise manner (interaction between one infectious and one healthy individuals) and (ii) to be caused by a single exposure of a healthy individual to an infectious one. Such processes of *simple contagion* can thus be conveniently represented by transmission mechanisms along the links of the network of contacts between individuals. Conversely, when dealing with social contagion phenomena, such as the adoption of norms, behaviours or new products, or the diffusion of rumors or fads, it is well known that simple contagion models do not provide a satisfactory description, while *complex contagion* mechanisms are required to account for the effects of peer influence [10]. Complex contagion can be broadly defined as a process in which multiple exposure to a stimulus is needed for the contagion to occur: for instance, in order to adopt a novel behavior, an individual needs to be convinced by a fraction of his/her social contacts larger than a given threshold [11]. Empirical evidence that complex contagion processes are more adequate than simple ones to describe social contagion have been provided in various contexts and experiments [12–16], and a number of models have been put forward to describe the resulting phenomenology [11, 14, 17–25]. All these models are, however, still defined on networks of interactions between individuals: even if multiple interactions might be needed for a contagion to take place, the fundamental building

blocks of the system are the pairwise interactions, as represented by the links of the network on which the process is taking place.

Here, we propose to go further and take into account that contagion can occur in different ways, either through pairwise interactions (links) or through group interactions, i.e., on higher-order structures. Indeed, while an individual can be convinced by each of his/her neighbors (simple contagion), or by the successive exposure to the arguments of different neighbors (complex contagion), a fundamentally different mechanism is at work if the neighbors of an individual form a group and convince him/her *in a group interaction*. For example, we can adopt a new norm because of two-body processes, which means we can get convinced, separately, by each one of our neighbors who have already adopted the norm. However, this is qualitatively different from a mechanism of contagion in which we get convinced because we are part of a social group of three individuals, and our two neighbors are both adopters. In this case the contagion is a three-body process that mimics the simplest multiple source of reinforcement that induces adoption. The same argument can easily be generalized to larger group sizes. To describe the co-existence of pairwise and higher-order interactions, simplicial representations are then more adapted than networks, as they characterize efficiently interactions between more than two units [26, 27]. We thus propose here a model of *simplicial contagion*, that is, a model for social contagion on simplicial complexes, which takes into account the fact that the processes and their rates can differ, depending on the fact that a contagion occurs on a link or is due to a group interaction. We do so by explicitly encoding the notion of groups into simplices and adopting simplicial complexes as the underlying structure of the social system under consideration. We recall that a k -simplex σ is in its simplest definition a collection of

* E-mail: i.iacopini@qmul.ac.uk

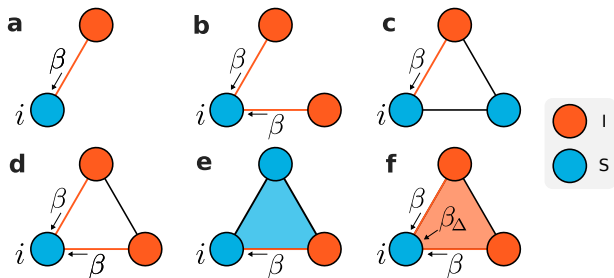


FIG. 1. Different channels of infection for a susceptible node i in the Simplicial Contagion Model (SCM) of order $D = 2$. Susceptible and infected nodes are colored in blue and red respectively. Node i is in contact with one (a, c) or more infected nodes (b, d) through a link (1-simplex), and for each one of these links is infected with probability β at each timestep. (e, f) Node i belongs to a 2-simplex (triangle). In (e) one of the nodes of the 2-simplex is not infected, so i can only receive the infection from the (red) link with probability β . In (f) the two other nodes of the 2-simplex are infected, so i can get the infection from each of the two 1-faces (links) of the simplex with probability β , and also from the 2-face with probability $\beta_2 = \beta_\Delta$.

$k - 1$ vertices $\sigma = [p_0, \dots, p_{k-1}]$. It is easy to see the difference between a group interaction among 3 elements (the “full” triangle $[p_0, p_1, p_2]$) and the collection of its edges ($[p_0, p_1], [p_0, p_2], [p_1, p_2]$). Just like a collection of edges defines a network, a collection of simplices (with an extra requirement) defines a simplicial complex: formally, a simplicial complex \mathcal{K} on a given set of vertices \mathcal{V} , with $|\mathcal{V}| = N$, is a collection of simplices, such that if a simplex $\sigma \in \mathcal{K}$, then all the subsimplices $\nu \in \sigma$ built from subsets of σ are also contained in \mathcal{K} . For simplicity and coherence with the standard network nomenclature, we call nodes (or vertices) the collection of 0-simplices, and links (or edges) the collection of 1-simplices of \mathcal{K} , while 2-simplices correspond to triangles, 3-simplices to tetrahedra and so on. Simplicial complexes, differently from networks, can thus efficiently characterize interactions between any number of units. Simplicial complexes are not a new idea [28], but thanks to the availability of new datasets and of recent advances in topological data analysis techniques [29], the interest in them has been renewed [27]. In particular, they recently proved to be particularly useful in describing the architecture of complex networks [30, 31] functional [32–34] and structural brain networks [35], semantic networks [36], and co-authorship networks in science [37].

The contagion model.—In order to model a simplicial contagion process, we associate a dynamical binary state variable x to each one of the N vertices of \mathcal{K} , such that $x_i(t) \in \{0, 1\}$ represents the state of vertex i at time t . By adopting a standard notation we divide the population of individuals into two classes of susceptible (S) and infectious (I) nodes, corresponding respectively to the values 0 and 1 of the state variable x . In the context e.g. of adoption process, the state I represents individuals who have adopted a behaviour. At each time t , the macroscopic or-

der parameter is given by the density of infectious nodes $\rho(t) = \frac{1}{N} \sum_{i=1}^N x_i(t)$. The model we propose here, the so-called *Simplicial Contagion Model (SCM) of order D* , with $D \in [1, N - 1]$, is governed by a set of D control parameters $B = \{\beta_1, \beta_2, \dots, \beta_D\}$, whose elements represent the probability per unit time for a susceptible node i that participates to a simplex σ of dimension D to get the infection from each one of the subfaces composing σ . In practice, with this notation, β_1 is equal to the standard probability of infection β that a susceptible node i gets the infection from an infected neighbor j through the link (i, j) (corresponding to the process $S + I \rightarrow 2I$). Similarly, the second parameter $\beta_2 \equiv \beta_\Delta$ corresponds to the probability per unit time that node i receives the infection from a closed triangle (2-simplex) (i, j, k) in which both j and k are infectious, $\beta_3 = \lambda_{\boxtimes}$ from a group of size 4 (3-simplex) to which it belongs, and so on. Such processes can be represented as $Simp(S, nI) \rightarrow Simp(I)$: a susceptible node, part of a simplex of $n+1$ nodes among which all other nodes are infectious, becomes infectious with probability per unit time β_n . Note that, thanks to the simplicial complex requirements that all subsimplices of a simplex are included, contagion processes in a n -simplex among which $p < n$ nodes are infectious are also automatically considered, each of the $n+1-p$ susceptible nodes being in simplices of size $p+1$ with the p infectious ones. Fig. 1 illustrates the concrete example of the six different channels of social contagion for an SCM of order $D = 2$ with parameters β and β_Δ . Finally, the recovery dynamics is controlled by the node-independent recovery probability μ ($I \rightarrow S$). Notice that the SCM of order D reduces to the standard SIS model on a network when $D = 1$, since in this case the infection can only be transmitted through the links of \mathcal{K} .

Numerical exploration of the model.—To explore the phenomenology of the simplicial contagion model, we consider synthetic simplicial complexes with controlled properties. A range of models for random simplicial complexes have been proposed so far, starting from the exponential random simplicial complex, the growing and generalized canonical ensemble [38–40] and the simplicial configuration models [41] to the more recent generalization of the activity driven temporal network model [42], the so called simplicial activity driven model [43]. While these yield Erdős-Rényi-like models [44, 45] of arbitrary complexity, here we are interested in models generating simplicial complexes with simplices of different dimension in which we can control the expected local connectivity (e.g. the number of edges and triangles a node belongs too). We define thus a new random simplicial complex (RSC) model, that allows us to keep the degree $\langle k_1 \rangle$ fixed, while controlling at the same time for the expected number of triangles. More precisely, the procedure works as follows. Given a set \mathcal{V} of N vertices we connect any two $i, j \in \mathcal{V}$ with probability p_1 , as in the Erdős-Rényi model [46], so that the average degree is $(N - 1)p_1$. Then, we add a 2-simplex (i, j, k) , for any $i, j, k \in \mathcal{V}$ with probability p_Δ . At this point each node has an average number

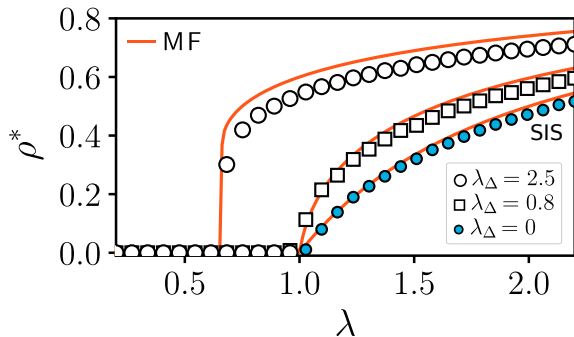


FIG. 2. SCM of order $D = 2$ on a synthetic random simplicial complex (RSC). The RSC is generated with the procedure described in this manuscript, with parameters $N = 2000$, p_1 and p_Δ tuned in order to produce a simplicial complex with $\langle k \rangle \sim 20$ and $\langle k_\Delta \rangle \sim 6$. The average fraction of infected obtained by means of numerical simulations is plotted against the rescaled infectivity $\lambda = \beta \langle k \rangle / \mu$ for $\lambda_\Delta = 0.8$ (white squares) and $\lambda_\Delta = 2.5$ (white dots). The blue dots denote the simulated curve for the equivalent standard SIS model ($\lambda_\Delta = 0$) that does not consider high-order effects, while the red lines stand for the analytical mean field solution, as described by Eq. (4). For $\lambda_\Delta = 2.5$ we observe a discontinuous (explosive) transition, with the formation of a bistable region where healthy and endemic states co-exist.

$\langle k_\Delta \rangle = (N - 1)(N - 2)p_\Delta/2$ of incident 2-simplices, and each contributes (in the sparse regime) to increase the degree of the node by 2 (since by definition a 2-simplex contains three 1-simplices). Finally, we can write the expected average degree $\langle k \rangle$ as the sum of these two contributions: $\langle k \rangle = (N - 1)p_1 + 2\langle k_\Delta \rangle$. For any given size N , we can thus produce simplicial complexes having desired values of $\langle k \rangle$ and $\langle k_\Delta \rangle$ by fixing p_1 and p_Δ as:

$$p_1 = \frac{\langle k \rangle - 2\langle k_\Delta \rangle}{N - 1} \quad (1a)$$

$$p_\Delta = \frac{2\langle k_\Delta \rangle}{(N - 1)(N - 2)} \quad (1b)$$

We simulate the SCM over a RSC created with the procedure described above, with $N = 2000$ nodes, with $\langle k \rangle \sim 20$ and $\langle k_\Delta \rangle \sim 6$. In particular, we stop each simulation if an absorbing state is reached, otherwise we compute the average stationary density of infectious ρ^* by averaging the values in the last 100 time-steps after reaching the stationary state. We then average over 100 runs obtained by starting with different randomly placed initial density of ρ_0 infectious and by using different RSCs.

Fig. 2 shows the average fraction of infected, as given by the simulations, as a function of the rescaled infectivity $\lambda = \beta \langle k \rangle$ for a SCM with $\lambda_\Delta = 0.8$ (white squares) and $\lambda_\Delta = 2.5$ (white dots). For comparison, we also plot the case $\lambda_\Delta = 0$, equivalent to the standard SIS model that does not consider high-order effects (blue dots). We observe two very different behaviour for the different values of λ_Δ : for $\lambda_\Delta = 0.8$, the density of infectious varies as a function of λ in a very similar way to the case $\lambda_\Delta = 0$

(simple contagion), with a continuous transition at $\lambda = 1$. For a large value of λ_Δ however, we observe a transition to an endemic state with $\rho^* > 0$ for values of λ below the epidemic threshold of the simple contagion model. Furthermore, this transition appears to be discontinuous (explosive), and an hysteresis loop appears in the region $\lambda^c < \lambda < 1$, where both healthy $\rho^* = 0$ and endemic $\rho^* > 0$ states can co-exist.

Mean field approach.—In order to study more extensively this phenomenology as λ_Δ and λ vary, and to further characterize the nature of the explosive transition, we consider a mean-field (MF) description of the SCM, under a homogeneous mixing hypothesis [47]. Given a recovery probability μ and a set of infection probabilities $B \equiv \{\beta_\omega\}$, we assume the independence between the states $x_i(t)$ and $x_j(t) \forall i, j$, and we write a MF expression for the temporal evolution of the density of infected nodes $\rho(t)$ as:

$$d_t \rho(t) = -\mu \rho(t) + \sum_{\omega=1}^D \beta_\omega \langle k_\omega \rangle \rho^\omega(t) [1 - \rho(t)] \quad (2)$$

where $k_\omega(i)$ is the generalized (simplicial) degree of a 0-dimensional face (node i), i. e. the number of ω -dimensional simplices incident to the node i [39, 40] and $\langle k_\omega \rangle$ its average over all the nodes $i \in \mathcal{V}$. With this approximation we assume that the local connectivity of the nodes is well described by globally averaged properties, such as the average generalized degree. We can immediately check that, if we consider only $D = 1$, we recover the standard MF equation for the SIS model that leads to the well known stationary state solutions $\rho_1^{*[D=1]} = 0$ and $\rho_2^{*[D=1]} = 1 - \mu/\beta \langle k \rangle$. Let us now focus on a more interesting but still analytically tractable case in which we limit the contagion dynamics up to dimension $D = 2$, so that Eq. (2) becomes:

$$d_t \rho(t) = -\mu \rho(t) + \beta \langle k \rangle \rho(t) [1 - \rho(t)] + \beta_\Delta \langle k_\Delta \rangle \rho^2(t) [1 - \rho(t)] \quad (3)$$

where $\langle k_\Delta \rangle = \langle k_{2,0} \rangle_i$. Defining $\lambda = \beta \langle k \rangle / \mu$ and $\lambda_\Delta = \beta_\Delta \langle k_\Delta \rangle / \mu$, and rescaling time by μ , we can rewrite Eq. (3) as:

$$d_t \rho(t) = -\rho(t)(\rho(t) - \rho_{2+}^*)(\rho(t) - \rho_{2-}^*) \quad (4)$$

with

$$\rho_{2(\pm)}^* = \frac{\lambda_\Delta - \lambda \pm \sqrt{(\lambda - \lambda_\Delta)^2 - 4\lambda_\Delta(1 - \lambda)}}{2\lambda_\Delta}. \quad (5)$$

The steady state equation $d_t \rho(t) = 0$ has thus up to three solutions in the acceptable range $\rho \in [0, 1]$. The solution $\rho_1^* = 0$ corresponds to the absorbing epidemic-free state, in which all the individuals recover and the spread dies out. The analysis of $\rho_{2(\pm)}^*$ shows that:

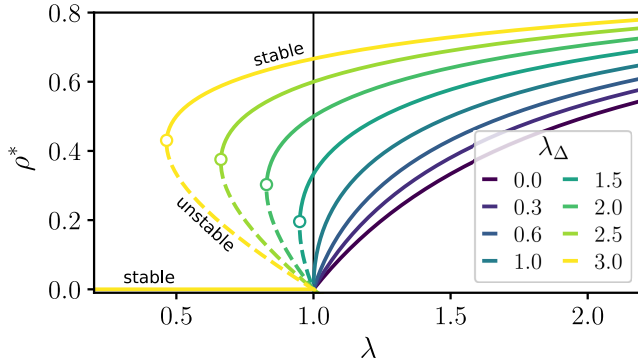


FIG. 3. Phase diagram of the SCM of order $D = 2$ in mean-field approximation. The stationary solutions ρ^* given by Eq. (5) are plotted as a function of the rescaled link infectivity $\lambda = \beta\langle k \rangle/\mu$. Different curves correspond to different values of the triangle infectivity $\lambda_\Delta = \beta_\Delta\langle k_\Delta \rangle/\mu$. Continuous and dashed lines correspond to stable and unstable branches respectively, while the vertical line denotes the epidemic threshold $\lambda^c = 1$ in the standard SIS model that does not consider high-order effects. For $\lambda_\Delta \leq 1$ the high order interactions contribute to increase the density of infected in the endemic state, while leaving the threshold unchanged. Contrarily, when $\lambda_\Delta > 1$ we observe a shift of the epidemic threshold, and the transition becomes discontinuous.

- if $\lambda_\Delta \leq 1$, $\rho_{2-}^* \leq 0$ and $\rho_{2+}^* \geq 0$ iff $\lambda \geq 1$. For $\lambda < 1$ therefore only the solution $\rho_1^* = 0$ exists, while for $\lambda \geq 1$ it becomes unstable ($d_t\rho(t)$ can be seen from Eq. (4) to be positive at small ρ) and the solution ρ_{2+}^* is stable. As $\rho_{2+}^* = 0$ for $\lambda = 1$, the transition at the epidemic threshold $\lambda = 1$ is continuous.
- if $\lambda_\Delta > 1$, ρ_{2+}^* exists and is positive for $\lambda > \lambda^c = 2\sqrt{\lambda_\Delta} - \lambda_\Delta$. For $\lambda^c < \lambda < 1$, $0 < \rho_{2-}^* < \rho_{2+}^*$ so that both $\rho_1^* = 0$ and ρ_{2+}^* are stable solutions while the solution ρ_{2-}^* is unstable: if $\rho(t=0) < \rho_{2-}^*$, Eq. (4) shows that $d_t\rho(t) < 0$ so that $\rho(t) \xrightarrow{t \rightarrow \infty} 0$, while, if $\rho(t=0)$ lies between ρ_{2-}^* and ρ_{2+}^* , $d_t\rho(t) > 0$ and $\rho(t) \xrightarrow{t \rightarrow \infty} \rho_{2+}^*$. For $\lambda > 1$ instead, $\rho_{2-}^* < 0 < \rho_{2+}^*$ so that $\rho_1^* = 0$ becomes unstable and ρ_{2+}^* is the only stable solution.

We illustrate these results by showing in Fig. 3 the solutions ρ_1^* and $\rho_{2(\pm)}^*$ as a function of λ and for different values of λ_Δ . The vertical line corresponds to the standard epidemic threshold for the SIS model ($\lambda_\Delta = 0$). Dashed lines depict the unstable branches as given by ρ_{2-}^* . We emphasize that for $\lambda_\Delta > 1$ we observe a discontinuous transition at $\lambda^c = 2\sqrt{\lambda_\Delta} - \lambda_\Delta$, instead of the usual continuous transition at the epidemic threshold, and the final state depends on the initial density of infectious for $\lambda^c < \lambda < 1$. We moreover show in Fig. 4 the 2-dimensional phase diagram for ρ_{2+}^* , where lighter regions correspond to higher values of the density of infectious, and the dashed vertical line corresponds to the epidemic threshold of the SIS model, $\lambda = 1$. For $\lambda_\Delta \leq 1$

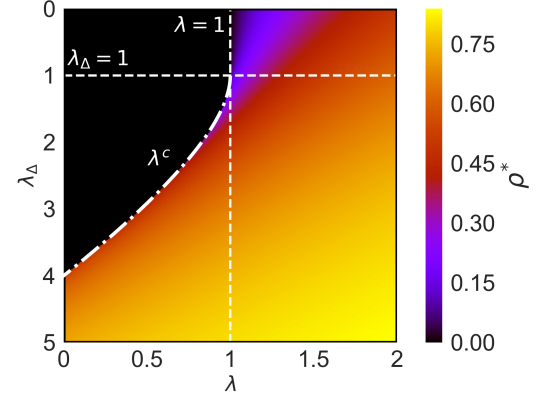


FIG. 4. Two-dimensional phase diagram of the SCM of order $D = 2$ in mean-field approximation. Heatmap of the stationary solution ρ^* (see Eq. 5) as a function of the rescaled infectivities $\lambda = \beta\langle k \rangle/\mu$ and $\lambda_\Delta = \beta_\Delta\langle k_\Delta \rangle/\mu$. The dashed vertical line corresponds to $\lambda = 1$, the epidemic threshold of the standard SIS model without high order effects. The dash-dotted line represents the curve $\lambda^c = 2\sqrt{\lambda_\Delta} - \lambda_\Delta$, highlighting the points in which the system undergoes a discontinuous transition.

(above the dashed horizontal line) the transition as λ crosses 1 is seen to be continuous, while, for $\lambda_\Delta > 1$, the transition is clearly seen as discontinuous along the curve $\lambda^c = 2\sqrt{\lambda_\Delta} - \lambda_\Delta$ (dash-dotted line). The analytical values of ρ_{2+}^* are also reported as continuous red lines in Fig. 2 and compared to the simulation results, showing in this way the accuracy of the MF approach just described. Notice that the MF is in fact able to correctly capture both the position of the thresholds and the explosive nature of the epidemic threshold for the SCM, for $\lambda_\Delta > 1$.

In summary, the simplicial model of social contagion introduced in this work is able to capture the basic mechanisms and effects of higher-order interactions in complex contagion processes. Although the results shown here are for nondescript simplicial complex (basically ER simplicial complexes), the framework we have introduced is very general. It would be interesting to investigate the SCM on simplicial complexes with heterogeneous generalized degree distribution or with community structure, and to consider simplicial complexes with emergent properties such as hyperbolic geometry [48], or temporally evolving simplicial complexes [43]. Furthermore we hope the idea will be extended from spreading processes to other dynamical systems, for instance to Kuramoto-like models with higher-order terms. Having such models might allow to disentangle higher-order dynamical effects in real data, which at the moment cannot be distinguished from standard network processes.

I. I. and V. L. acknowledge support from EPSRC Grant EP/N013492/1. I. I. acknowledges support from The Alan Turing Institute under the EPSRC Grant No. EP/N510129/1, and G. P. from ADnD Grant by Compagnia San Paolo.

-
- [1] R. Albert and A.-L. Barabási, *Rev. Mod. Phys.* **74**, 47 (2002).
- [2] V. Latora, V. Nicosia, and G. Russo, *Complex Networks: Principles, Methods and Applications* (Cambridge University Press, 2017).
- [3] M. A. Porter and J. P. Gleeson, *Dynamical systems on networks: A tutorial* (Springer, 2005).
- [4] A. Barrat, M. Barthelemy, and A. Vespignani, *Dynamical processes on complex networks* (Cambridge university press, 2008).
- [5] R. Pastor-Satorras, C. Castellano, P. Van Mieghem, and A. Vespignani, *Rev. Mod. Phys.* **87**, 925 (2015).
- [6] T. W. Valente, *Comp. Math. Org. Th.* **2**, 163 (1996).
- [7] R. Cowan and N. Jonard, *J. Econ. Dyn. Control* **28**, 1557 (2004).
- [8] I. Iacopini, S. Milojević, and V. Latora, *Phys. Rev. Lett.* **120**, 048301 (2018).
- [9] D. J. Watts and P. S. Dodds, *J. Consum. Res.* **34**, 441 (2007).
- [10] D. Guilbeault, J. Becker, and D. Centola, in *Complex Spreading Phenomena in Social Systems* (Springer, 2018) pp. 3–25.
- [11] D. J. Watts, *Pro. Natl. Acad. Sci. U.S.A.* **99**, 5766 (2002).
- [12] D. Centola, *Science* **329**, 1194 (2010).
- [13] J. Ugander, L. Backstrom, C. Marlow, and J. Kleinberg, *Pro. Natl. Acad. Sci. U.S.A.* , 201116502 (2012).
- [14] L. Weng, A. Flammini, A. Vespignani, and F. Menczer, *Sci. Rep.* **2**, 335 (2012).
- [15] M. Karsai, G. Iniguez, K. Kaski, and J. Kertész, *J. R. Soc. Interface* **11**, 20140694 (2014).
- [16] B. Mønsted, P. Sapiezynski, E. Ferrara, and S. Lehmann, *PLoS One* **12**, e0184148 (2017).
- [17] D. Centola and M. Macy, *Americ. J. Sociol.* **113**, 702 (2007).
- [18] S. Melnik, J. A. Ward, J. P. Gleeson, and M. A. Porter, *Chaos* **23**, 013124 (2013).
- [19] E. Cozzo, R. A. Banos, S. Meloni, and Y. Moreno, *Phys. Rev. E* **88**, 050801 (2013).
- [20] N. O. Hodas and K. Lerman, *Sci. Rep.* **4**, 4343 (2014).
- [21] M. Herrera, G. Armelini, and E. Salvaj, *PLoS One* **10**, e0140891 (2015).
- [22] D. J. O’Sullivan, G. J. O’Keeffe, P. G. Fennell, and J. P. Gleeson, *Front. Phys.* **3**, 71 (2015).
- [23] Z. Ruan, G. Iniguez, M. Karsai, and J. Kertész, *Phys. Rev. Lett.* **115**, 218702 (2015).
- [24] A. Czaplicka, R. Toral, and M. San Miguel, *Phys. Rev. E* **94**, 062301 (2016).
- [25] P. Tuzón, J. Fernández-Gracia, and V. M. Eguíluz, *Front. Phys.* **6**, 21 (2018).
- [26] A. Hatcher, *Algebraic topology* (2002).
- [27] V. Salnikov, D. Cassese, and R. Lambiotte, arXiv preprint arXiv:1807.07747 (2018).
- [28] P. S. Aleksandrov, *Combinatorial topology*, Vol. 1 (Courier Corporation, 1998).
- [29] G. Carlsson, *Bull. Am. Math. Soc.* **46**, 255 (2009).
- [30] G. Petri, M. Scolamiero, I. Donato, and F. Vaccarino, *PLoS One* **8**, e66506 (2013).
- [31] A. Sizemore, C. Giusti, and D. S. Bassett, *J. Comp. Net.* **5**, 245 (2016).
- [32] G. Petri, P. Expert, F. Turkheimer, R. Carhart-Harris, D. Nutt, P. J. Hellyer, and F. Vaccarino, *J. Royal Soc. Interface* **11**, 20140873 (2014).
- [33] L.-D. Lord, P. Expert, H. M. Fernandes, G. Petri, T. J. Van Hartevelt, F. Vaccarino, G. Deco, F. Turkheimer, and M. L. Kringelbach, *Front. Syst. Neurosci.* **10**, 85 (2016).
- [34] H. Lee, H. Kang, M. K. Chung, B.-N. Kim, and D. S. Lee, *IEEE Trans. Med. Imaging.* **31**, 2267 (2012).
- [35] A. E. Sizemore, C. Giusti, A. Kahn, J. M. Vettel, R. F. Betzel, and D. S. Bassett, *J. Comp. Neurosci.* **44**, 115 (2018).
- [36] A. E. Sizemore, E. A. Karuza, C. Giusti, and D. S. Bassett, arXiv preprint arXiv:1709.00133 (2017).
- [37] A. Patania, G. Petri, and F. Vaccarino, *EPJ Data Sci.* **6**, 18 (2017).
- [38] K. Zuev, O. Eisenberg, and D. Krioukov, *J. Phys. A* **48**, 465002 (2015).
- [39] O. T. Courtney and G. Bianconi, *Phys. Rev. E* **93**, 062311 (2016).
- [40] O. T. Courtney and G. Bianconi, *Phys. Rev. E* **95**, 062301 (2017).
- [41] J.-G. Young, G. Petri, F. Vaccarino, and A. Patania, *Phys. Rev. E* **96**, 032312 (2017).
- [42] N. Perra, B. Gonçalves, R. Pastor-Satorras, and A. Vespignani, *Sci. Rep.* **2**, 469 (2012).
- [43] G. Petri and A. Barrat, arXiv preprint arXiv:1805.06740 (2018).
- [44] M. Kahle, *Discrete Mathematics* **309**, 1658 (2009).
- [45] A. Costa and M. Farber, in *Configuration Spaces* (Springer, 2016) pp. 129–153.
- [46] P. Erdos and A. Rényi, *Publ. Math. Inst. Hung. Acad. Sci* **5**, 17 (1960).
- [47] I. Z. Kiss, J. C. Miller, P. L. Simon, *et al.*, Cham: Springer (2017).
- [48] G. Bianconi and C. Rahmede, *Sci. Rep.* **7**, 41974 (2017).